

UDK 661.834:519.785:661.883

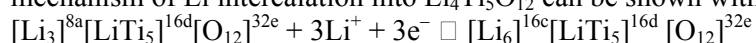
Solid State Synthesis of Extra Phase-Pure $\text{Li}_4\text{Ti}_5\text{O}_{12}$ Spinel**I. Veljković^{1*}, D. Poletić², Lj. Karanović³, M. Zdujić⁴, G. Branković⁵**¹Innovation Center, Faculty of Technology & Metallurgy, University of Belgrade, Karnegijeva 4, 11000 Belgrade, Serbia²Department of General and Inorganic Chemistry, Faculty of Technology and Metallurgy, University of Belgrade, Karnegijeva 4, 11000 Belgrade, Serbia³Laboratory of Crystallography, Faculty of Mining and Geology, University of Belgrade, Đušina 7, 11000 Belgrade, Serbia⁴Institute of Technical Sciences of the Serbian Academy of Sciences and Arts, 11000 Belgrade, Knez Mihailova 35, 11000 Belgrade, Serbia⁵Institute for Multidisciplinary Studies, University of Belgrade, Kneza Višeslava 1, 11000 Belgrade, Serbia**Abstract:**

Extra phase-pure $\text{Li}_4\text{Ti}_5\text{O}_{12}$ spinel with particle sizes less than 500 nm was synthesized by solid state reaction of mechanochemically activated mixture of nano anatase and Li_2CO_3 for a very short annealing time, 4 h at 800 °C. Structural and microstructural properties, the mechanism of solid state reaction between anatase and Li_2CO_3 as well as thermal stability of prepared spinel were investigated using XRPD, SEM and TG/DSC analysis. The mechanism of reaction implies decomposition of Li_2CO_3 below 250 °C, formation of monoclinic Li_2TiO_3 as intermediate product between 400 and 600 °C and its transformation to $\text{Li}_4\text{Ti}_5\text{O}_{12}$ between 600–800 °C. The spinel structure is stable up to 1000 °C when it is decomposed due to Li_2O evaporation.

Keywords: X-ray diffraction, Mechanism, Thermal stability, $\text{Li}_4\text{Ti}_5\text{O}_{12}$, Spinel, Phase-pure

1. Introduction

Lithium titanate, $\text{Li}_4\text{Ti}_5\text{O}_{12}$, was presented in the 1990s as a prospective “zero-strain” Li-insertion material [1-3]. “Zero-strain” insertion of lithium considers that there is a negligible expansion and contraction of the material during intercalation/elimination of Li^+ ions. $\text{Li}_4\text{Ti}_5\text{O}_{12}$ has a spinel structure (space group $\text{Fd}\bar{3}m$, $a \approx 8.35 \text{ \AA}$) that consists of a nearly cubic closed pack of oxygen atoms with lithium atoms occupying tetrahedral (8a) and octahedral (16c, 16d) sites, whereas Ti, partly substituted by Li, is placed in the octahedral 16d sites. The overall Li-insertion capacity is limited by the number of free octahedral sites, but $\text{Li}_4\text{Ti}_5\text{O}_{12}$ can accommodate 3Li^+ per unit cell with no change of unit cell parameter a . The mechanism of Li intercalation into $\text{Li}_4\text{Ti}_5\text{O}_{12}$ can be shown with the following equation:



The intercalation/elimination process is based on the phase transition of spinel structured $\text{Li}_4\text{Ti}_5\text{O}_{12}$ to NaCl structured $\text{Li}_7\text{Ti}_5\text{O}_{12}$, permitting in that manner the reduction of 3Ti^{4+} ions out of 5, which corresponds to the theoretical capacity of 175 Ah kg^{-1} .³ Detailed

*) **Corresponding author:** ivana@tmf.bg.ac.rs

studies about chemical and electrochemical Li-insertion into $\text{Li}_4\text{Ti}_5\text{O}_{12}$ were performed by Aldon et al. [4] and Ariyoshi et al. [5]. The phase transition occurs without or with a very small displacement of oxygen atoms from their original positions in the spinel structure. The negligible structural changes during lithium insertion/extraction make $\text{Li}_4\text{Ti}_5\text{O}_{12}$ an advanced anode material for long-cycle life battery applications. Furthermore, in comparison to natural graphite, $\text{Li}_4\text{Ti}_5\text{O}_{12}$ shows better thermal stability and sharper voltage wave that can serve as an overcharge/discharge indicator [6]. On the other hand, a phase-pure $\text{Li}_4\text{Ti}_5\text{O}_{12}$, appropriate for anode application in Li-ion batteries, is difficult to prepare. The main reason is that annealing time and temperature are restricted in order to inhibit particles growth and to maintain good electrochemical properties [7].

Syntheses of $\text{Li}_4\text{Ti}_5\text{O}_{12}$ spinel mainly by the sol-gel technique have been studied extensively [8-10]. Although many authors claim about low temperature sol-gel spinel synthesis, it was not difficult to notice that prepared samples were not really a phase-pure until long annealing times (often more than 12 h) at temperatures about or above 800 °C were applied. Because sol-gel routes could be tedious and often require toxic and/or expensive reactants, it seems that solid-state reactions are an enhanced approach for synthesis of this material. Until now, Ohzuku et al. [3] obtained a phase-pure $\text{Li}_4\text{Ti}_5\text{O}_{12}$ by annealing $\text{LiOH}\cdot\text{H}_2\text{O}$ and anatase powder mixture at 800 °C for 12 h, while Birke et al. [11] synthesized the spinel from a mixture of Li_2CO_3 and rutile at 850 °C for 24 h. Guerfi et al. were successfully prepared a phase-pure $\text{Li}_4\text{Ti}_5\text{O}_{12}$ by heating a ball-milled solid Li_2CO_3 -anatase mixture at 850 °C for 12 h [12]. Abe et al. made efforts to prepare a phase-pure $\text{Li}_4\text{Ti}_5\text{O}_{12}$ from the same mixture using short annealing times (1 – 3 h), but temperature about 950 °C was necessary to obtain 81 – 88 % phase purity [13]. Wang et al. synthesized $\text{Li}_4\text{Ti}_5\text{O}_{12}$ by high energy ball milling (HEBM) of a mixture containing $\text{LiOH}\cdot\text{H}_2\text{O}$ and anatase with subsequent annealing at 800 °C for 12 h and investigated the influence of milling time on morphology and electrochemical properties [14]. Although the resulted particles were not small enough, the effects of mechanical activation are supportive for lowering the annealing temperature, and HEBM is a very promising way to produce micro- or even nanostructured $\text{Li}_4\text{Ti}_5\text{O}_{12}$ spinel and similar materials.

In this work we report the synthesis of extra phase-pure $\text{Li}_4\text{Ti}_5\text{O}_{12}$ via solid state route by annealing a HEBM activated Li_2CO_3 -anatase mixture for only 4 h at 800 °C. Also, the influence of TiO_2 particle size on the reaction, thermal properties and powder morphology of the products were examined.

2. Experimental

Two powder mixtures with a molar ratio of Li : Ti = 4 : 5, distinctive by particle size of starting TiO_2 , were studied. The British Drug Houses Ltd. Li_2CO_3 was used as the lithium source in a combination with micro or nano sized TiO_2 (anatase). The average particle size of Fluka micro sized anatase was about 7 μm (as measured by the particle size analyzer Mastersizer 2000), while Aldrich nano anatase was declared by manufacturer as less than 5 nm. The mixtures were treated by HEBM using the SFM-1 High Speed Shimmy Ball Mill (MTI Corporation) in stainless steel vials of 250 ml volume for 4 h. Powder ($m = 10$ g) to balls ($d = 13.4$ mm) mass ratio was 1:30. The angular velocity of vials was 396 rpm for first 2 h and 550 rpm for second 2 h of milling. The mechanically activated mixtures were subsequently annealed at 400, 600 and 800 °C for 4 h in air, and spontaneously furnace cooled to room temperature.

X-ray powder diffraction data (XRPD) were collected on an Ital Structures APD2000 diffractometer, while phase composition of samples was completed using the Powder Cell 2.4 program [15]. The mean crystallite size, $\langle D \rangle$, of the initial TiO_2 nanopowder and milled samples was estimated by the Scherrer formula [16] from the highest (101) anatase maximum

at $25.35^\circ 2\theta$. The peak widths were corrected for instrumental broadening using LaB_6 as a standard material. The thermal behavior of the precursor mixture and final products was studied using an SDT Q600 TGA/DSC instrument (TA Instruments) up to 1200°C at a heating rate of $20^\circ\text{C min}^{-1}$ under a dynamic air atmosphere (flow-rate $100\text{ cm}^3\text{ min}^{-1}$). The morphology of powders was investigated by Vega–Tescan VEGA TS 51 30MM scanning electron microscope.

3. Results And Discussion

3.1 Structural and microstructural properties

Figs. 1 and 2 show the evolution of the spinel $\text{Li}_4\text{Ti}_5\text{O}_{12}$ structure originated from the HEBM mixtures of Li_2CO_3 with micro (sample mALi) and nano anatase (sample nALi), respectively. Already after the mechanochemical treatments a slightly different behavior of the samples, especially regarding crystallinity of anatase phase, was observed (Figs. 1a and 2a). While Li_2CO_3 phase is almost completely amorphized in both cases, the estimated mean crystallite size, $\langle D \rangle$, of anatase phases are: 13, 14 and 30 nm, for the initial nano anatase, nALi and mALi, respectively. Thus, milling had no significant effect on nano anatase, probably because the initial size of crystallites was below the limit of possible milling efficiency for given experimental conditions.

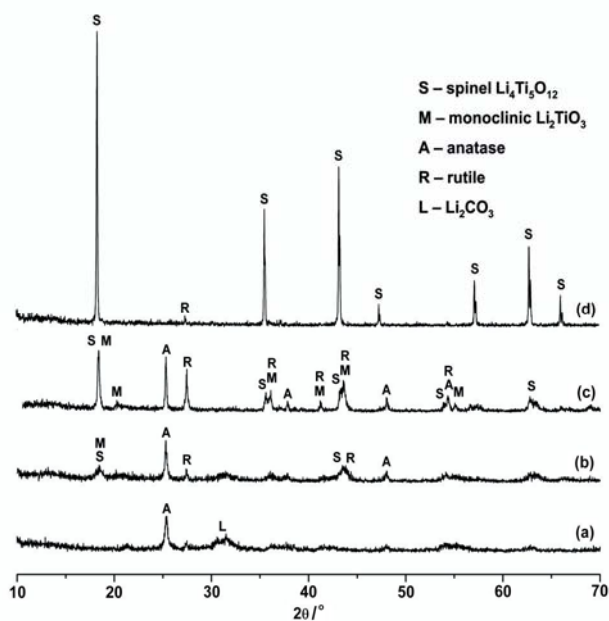


Fig. 1. XRPD patterns of the mALi sample after: (a) HEBM treatment and annealing at (b) 400°C , (c) 600°C , and (d) 800°C

Microstructural characteristics of as-milled samples are practically identical and only micrographs of nALi sample are shown in Figs. 3a and 3b. After milling, the powders consist of irregular agglomerates ranging from 1 to $20\ \mu\text{m}$ that are formed from particles of very different shape and size (from less than $100\ \text{nm}$ to about $1\ \mu\text{m}$). This is typical for most HEBM samples, see, for examples [17-19].

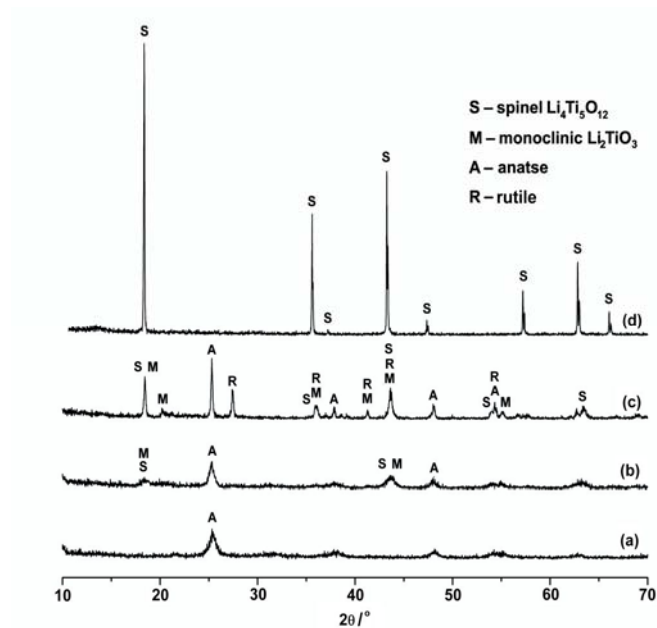


Fig. 2. XRPD patterns of the nALi sample after: (a) HEBM treatment and annealing at (b) 400 °C, (c) 600 °C, and (d) 800 °C

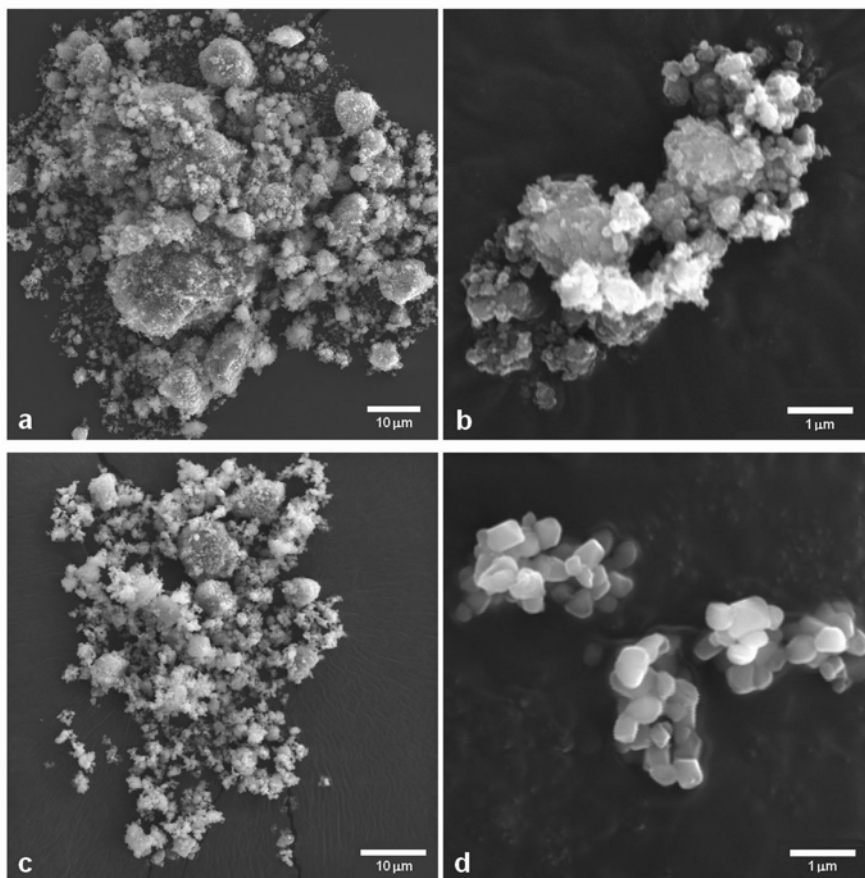


Fig. 3. SEM of the nALi sample: after milling (a and b) and after annealing at 800 °C (c and d)

Annealing at 400 °C (Figs. 1b and 2b) resulted in appearance of a Li-containing phase;

besides, a slight anatase to rutile transition (authenticated by a small rutile peak at $27.4^\circ 2\theta$) was observed in the mALi sample. The maxima of Li-containing phase correspond to the $\text{Li}_4\text{Ti}_5\text{O}_{12}$ spinel (JCPDS card 82-1616), but also to the monoclinic Li_2TiO_3 phase (JCPDS card 88-0416), and in this stage of the reaction the structure was not enough developed for reliable concluding. After annealing at 600°C the shape of peak at $18.3^\circ 2\theta$ and partial splitting of peak at $43.3^\circ 2\theta$ confirmed the presence of both $\text{Li}_4\text{Ti}_5\text{O}_{12}$ and Li_2TiO_3 phase (Figs. 1c and 2c). Similar behavior was already noticed by many authors in related systems [20-22].

The phase composition of the samples after annealing at 600°C , Tab. I, show another dissimilarity between two systems, particularly when contents of monoclinic and spinel phase are compared. Such behavior indicates different kinetics and/or mechanism of the reactions depending on particle size of anatase used (vide infra).

Tab. I. Phase composition of the samples after annealing at 600°C

Sample	Phase composition / mass %			
	Anatase (A)	Rutile (R)	Li_2TiO_3 (M)	$\text{Li}_4\text{Ti}_5\text{O}_{12}$ (S)
mALi	16	20	35	29
nALi	23	19	49	9

Contrary to the four-phases systems obtained at 600°C , calcination at 800°C resulted in formation of the phase-pure $\text{Li}_4\text{Ti}_5\text{O}_{12}$ samples (Figs. 1d and 2d). Actually, a careful analysis and comparison of diffractograms has shown traces of rutile impurity (about 1 mass %) in the final mALi sample (Fig. 1d). On the other hand, rutile peaks were not observed in the case of nALi sample (Fig. 2d) demonstrating the presence of an extra phase-pure $\text{Li}_4\text{Ti}_5\text{O}_{12}$ spinel and advantage of nano anatase as starting material. The unit cell parameters of the prepared spinels calculated by the program LSUCRIPC [23] are: $8.359(1)\text{ \AA}$ for both prepared samples.

Although single phase samples were prepared by many authors at temperatures about 800°C , it was necessary to apply long annealing times, so there is a general agreement about difficulty to obtain phase-pure samples with no traces of anatase or rutile [11,12,24]. In addition to the obvious effect of nano anatase, a two-stage milling (see Experimental) could also be of some importance in our procedure, because even in the final mALi sample the rutile content is almost negligible.

Scanning electron micrographs revealed very different powder morphologies of milled and annealed samples (Fig. 3). After annealing particles have very similar shape with sizes less than 500 nm and they form smaller agglomerates. No sintering effects could be observed, and it was not possible to detect rutile impurities in mALi sample. As noticed by many authors, $\text{Li}_4\text{Ti}_5\text{O}_{12}$ particles could stay relatively small if short annealing times are applied [13,30]. Also, $\text{Li}_4\text{Ti}_5\text{O}_{12}$ with very similar particle sizes have very good electrochemical properties and some authors suggested that the solid-state method is suitable for the preparation of anode material with high discharge capacity, excellent good cycling behavior and rate property [25,26].

3.2. Thermal properties, mechanism and kinetics of reaction

In order to get deeper insight into mechanism of solid state reaction between Li_2CO_3 and TiO_2 milled nALi precursor was additionally examined by TG/DSC analysis from room temperature to 1200°C (Fig. 4). Generally, the TG/DSC results are in a good agreement with

previously published studies on $\text{Li}_4\text{Ti}_5\text{O}_{12}$ precursors prepared by HEBM [27,28] or even by sol-gel technique [29-31]. The main mass loss of 20.7 % occurs in two highly endothermic and overlapped steps between room temperature and 500 °C. As shown by inflection point at 250 °C, the accompanied mass losses are 8.4 %, for the first, and 12.3 %, for the second step. The first step is comparable to the results for mechanochemically activated powder mixtures that include Li_2CO_3 and can be attributed to the vaporization of air moisture entered during HEBM [27,28]. However, the mass loss during the second step is smaller than theoretical value (16.1 mass %) if only escape of CO_2 from Li_2CO_3 is assumed. This means that decomposition of Li_2CO_3 starts even below 250 °C, which is much lower than 380 °C as observed for non-activated mixtures containing Li_2CO_3 [28].

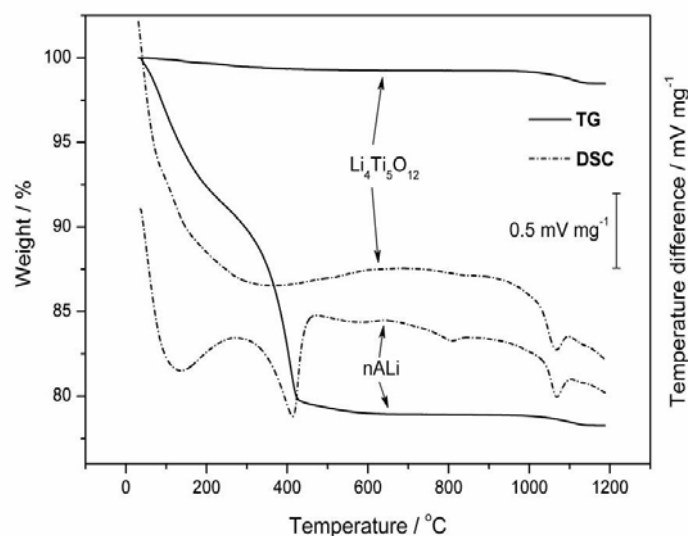
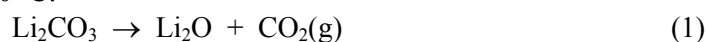


Fig. 4. TG/DSC curves of nALi sample after milling and final nALi spinel

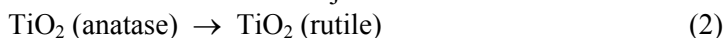
Between 500 and 1000 °C the process continues with a negligible mass loss (about 1 %), but two weak and broad endothermic peaks centered at 582 and 809 °C are visible. Considering the results of XRPD analysis (Table I), the first peak probably implies formation of monoclinic Li_2TiO_3 and simultaneous anatase \rightarrow rutile phase transition. Then the second peak could represent the ending reaction between Li_2TiO_3 and an excess of TiO_2 giving the spinel $\text{Li}_4\text{Ti}_5\text{O}_{12}$ phase.

After the reaction is finished at about 800 °C, $\text{Li}_4\text{Ti}_5\text{O}_{12}$ is thermally stable up to approximately 1000 °C, where a small mass loss (0.6 %) indicated a slight evaporation of Li_2O . Similar effect has been noticed by several authors for Li-containing spinel systems, [32,33] but to our knowledge it was never investigated in detail. Because of that, the nALi precursor was heated at 1150 °C for 2 h, cooled and analyzed by XRPD, which confirmed the presence of at least four phases. Two of them predominate: $\text{Li}_{2.03}\text{Ti}_{3.43}\text{O}_8$ (ICSD Collection Code 202897) and $\text{Li}_4\text{Ti}_5\text{O}_{12}$, but a minor quantity of rutile was also found. Besides, several broad XRPD peaks at 3.90, 2.56 and 1.80 Å indicated the presence of a low crystalline and unknown phase(s). Thus, the occurrence of phases with lower Li content, $\text{Li}_{2.03}\text{Ti}_{3.43}\text{O}_8$ and rutile, confirms the evaporation of Li_2O .

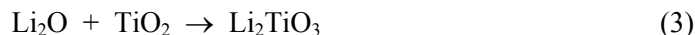
From previous discussion the following mechanism of the formation of $\text{Li}_4\text{Ti}_5\text{O}_{12}$ in the investigated system can be assumed. The overall process starts with decomposition of the amorphous Li_2CO_3 well below 250 °C:



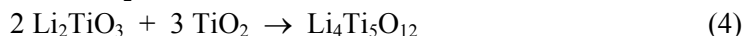
which is immediately followed by a very slow formation of a Li-containing, very likely the monoclinic Li_2TiO_3 , phase. Between 400 and 600 °C two major reactions are:



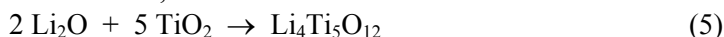
and



where TiO_2 is either anatase or rutile TiO_2 modification. Above 600 °C the main reaction is:

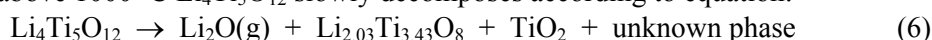


and it is completed at about 800 °C. Of course, a direct reaction:



should not be neglected. However, from data given in Table I this reaction does not look very probable, especially in the case of nALi sample. Therefore, the monoclinic Li_2TiO_3 is a very important intermediate in the solid state synthesis of $\text{Li}_4\text{Ti}_5\text{O}_{12}$.

Finally, above 1000 °C $\text{Li}_4\text{Ti}_5\text{O}_{12}$ slowly decomposes according to equation:



When the phase composition of samples after annealing at 600 °C (Table I) is taken into account, it can be concluded that reaction 4 and/or 5 starts under 600 °C, and it is much faster in the case of mALi sample. At the same time, in the 400–600 °C range reaction 3 predominates in the case of nALi sample. Together with the fact that the rutile to anatase ratio is higher in the mALi sample (1.25 versus 0.82, for mALi and nALi sample, respectively), this can give a tentative explanation why traces of rutile are found in the final mALi sample. Namely, rutile has a much lower reactivity with lithium than anatase, particularly when it is not nanosized [34,35]. That means that formation of rutile requires higher temperature (or longer time) of calcination, so an earlier formation of rutile when micro anatase is used probably is the essential factor for different behavior of these two systems. A higher reactivity of nano anatase with lithium (comparing to micro anatase) retards anatase to rutile transformation giving the privilege to lithiation at temperatures higher than 600 °C.

4. Conclusions

Extra phase-pure $\text{Li}_4\text{Ti}_5\text{O}_{12}$ spinel was synthesized by solid state reaction of anatase and lithium carbonate for a very short annealing time, 4 h at 800 °C. The mechanism of the reaction implies decomposition of Li_2CO_3 to Li_2O and CO_2 below 250 °C, formation of the monoclinic Li_2TiO_3 phase between 400 and 600 °C and its further reaction with TiO_2 to form $\text{Li}_4\text{Ti}_5\text{O}_{12}$ in the range 600–800 °C. Of course, a parallel direct reaction between Li_2O and TiO_2 should not be denied.

Phase purity of $\text{Li}_4\text{Ti}_5\text{O}_{12}$ generally depends on the kinetic of anatase to rutile transformation hence rutile is less reactive with lithium. When nano anatase is used as reactant its transformation to rutile occurs at higher temperature than in mALi sample, leading to extra pure phase $\text{Li}_4\text{Ti}_5\text{O}_{12}$ after shorter annealing time than usual. Two step HEBM treatment is probably important factor leading to the spinel phase purity, since even in final mALi sample the impurities content was almost negligible.

Prepared spinels have particle sizes of less than 500 nm due to short annealing time and are stable to about 1000 °C when a slight Li_2O evaporation is occurred, during which spinel structure decomposes into several phases with lower Li content and rutile.

Acknowledgments

The Ministry of Science and Technological Development of the Republic of Serbia, Grants No. 45007, supported this work.

References

1. K.M. Colbow, J.R. Dahn, P.R. Haering, *J. Power Sources* 26 (1989) 397.
2. E. Ferg, R. J. Gummov, A. de Kock, *J. Electrochem. Soc.* 141 (1994) L147.
3. T. Ohzuku, A. Ueda, N. Yamamoto, *J. Electrochem. Soc.* 142 (1995) 1431.
4. L. Aldon, P. Kubiak, M. Womes, J. C. Jumas, J. Olivier-Fourcade, J. L. Tirado, J. I. Corredor, C. Perez Vicente, *Chem. Mater.* 16 (2004) 5721.
5. K. Ariyoshi, R. Yamato, T. Ohzuku, *Electroch. Acta* 51 (2005) 1125.
6. L. Yao, S. Xie, C.H. Chen, Q.S. Wang, J.H. Sun, Y.L. Li, S.X. Lu, *Electroch. Acta* 50 (2005) 4076.
7. M. Kalbáč, M. Zukalová, L. Kavan, *J. Solid State Electr.* 8 (2003) 2.
8. Y.H. Rho, K. Kanamura, M. Fujisaki, J. Hamagami, S. Suda, T. Umegaki, *Solid State Ionics* 151 (2002) 151.
9. Y.H. Rho, K. Kanamura, *J. Electrochem. Soc.* 151 (2004) A106.
10. K. Kanamura, N. Akutagawa, K. Dokko, *J. Power Sources* 146 (2005) 86.
11. P. Birke, F. Salam, S. Doring, W. Weppner, *Solid State Ionics* 118 (1999) 149.
12. A. Guerfi, P. Charest, K. Konoshita, M. Perrier, K. Zaghbi, *J. Power Sources* 126 (2004) 163.
13. Y. Abe; E. Matsui, M. Senna, *J. Phys. Chem. Solids*, 68 (2007) 681.
14. G. Wang; J. Xu; M. Wen; R. Cai; R. Ran, Z. Shao, *Solid State Ionics*, 179 (2008) 946.
15. W. Kraus, G. Nolze, *PowderCell for Windows, V2.4*, Federal Institute for Materials Research and Testing, Berlin, Germany, 2000.
16. H.P. Klug, L.E. Alexander, *X-ray diffraction procedures*, 2nd ed., Wiley, New York, 1974, p. 687.
17. I. Veljkovic, D. Poleti, M. Zdujic, Lj. Karanovic, Č. Jovalekic, *Materials Letters* 62 (2008) 2769.
18. Q. Zhang, T. Nakagawa, F. Saito, *J. Alloy. Compd.* 308 (2000) 121.
19. P.P. Chin, J. Ding, J.B. Yi, B.H. Liu, *J. Alloy. Compd.* 390 (2005) 255.
20. E. Matsui, Y. Abe, M. Senna, A. Guerfi, K. Zaghbi, *J. Am. Ceram. Soc.* 91 (2008) 1522.
21. J. Grabis, A. Orlovs, Dz. Rasmene, *Functional Materials And Nanotechnologies*, (2007), Riga, Latvia, 2007, p. 012004.
22. M. Mohammadi, D. Fray, *J. Sol-Gel Sci. Techn.* 55 (2010) 19.
23. R.G. Garvey, LSUCRI Least Squares Unit Cell Refinement for the Personal Computer, *Powder Diffr.* 1 (1986) 114.
24. P. Proisini, R. Mancini, L. Petrucci, V. Contini, P. Villano, *Solid State Ionics* 144 (2001) 185.
25. Y. Guo-Feng, L. Guang-She, L. Li-Ping, F. Hai-Sheng, *Chinese J. Struct. Chem.* 28 (2009) 1393.
26. K. Nakahara, R. Nakajima, T. Matsushima, H. Majima, *J. Power Sources* 117 (2003) 131.
27. M. Ganesan, M. Dhananjeyan, K. Sarangapani, N. Renganathan, *J. Electroceram.* 18 (2007) 329.
28. V. Berbenni, A. Marini, *J. Anal. Appl. Pyrol.* 70 (2003) 437.
29. C. Shen, X. Zhang, Y. Zhou, H. Li, *Mater. Chem. Phys.* 78 (2003) 437.
30. D. Wang, N. Ding, X. Song, C. Chen, *J. Mater. Sci.* 44 (2009) 198.
31. M.W. Raja, S. Mahanty, M. Kundu, R. N. Basu, *J. Alloy. Compd.* 468 (2009) 258.
32. E. Antolini, *J. Mater. Sci. Lett.* 13 (1994) 1599.
33. E. Antolini, M. Ferretti, *J. Solid State Chem.*, 117 (1995) 1.

-
34. W.J.H. Borghols, M. Wagemaker, U. Lafont, E.M. Kelder, F.M. Mulder, Chem. Mater. 20 (2008) 2949.
35. Z. Yang, D. Choi, S. Kerisit, K. M. Rosso, D. Wang, J. Zhang, G. Graff, J. Liu, J. Power Sources 192 (2009) 588.

Садржај: Фазно чист спинел $\text{Li}_4\text{Ti}_5\text{O}_{12}$ са величином честица мањом од 500 nm добијен је реакцијом у чврстом стању из стехиометријске смеше наноанатаса (TiO_2) и Li_2CO_3 која је претходно активирана механохемијским поступком. Реакција у чврстом стању у потпуности се завршава за само 4 часа на температури од 800 °C. Уз помоћ XRPD, SEM и TG/DSC анализе испитане су структурне и микроструктурне карактеристике добијеног спинела, механизам реакције између анатаса и Li_2CO_3 , као и термичка стабилност $\text{Li}_4\text{Ti}_5\text{O}_{12}$. Реакција започиње разлагањем Li_2CO_3 на температурама нижим од 250 °C. Након тога, на температурама између 400 и 600 °C долази до формирања моноклиничног Li_2TiO_3 као интермедијарног производа, док спинел, $\text{Li}_4\text{Ti}_5\text{O}_{12}$ настаје у интервалу од 600 до 800 °C. Спинел је стабилан до 1000 °C, а затим долази до његовог разлагања услед испаравања Li_2O .

Кључне речи: спинел, $\text{Li}_4\text{Ti}_5\text{O}_{12}$, рендгенска дифракција, механизам реакције, термичка стабилност
